An analysis of the ECRF stray radiation in JT-60SA

C.Sozzi[1], L. Figini[1], D. Farina[1], D. Micheletti[1], A.Moro[1], P.Platania[1], D.Ricci[1], T.Kobayashi[2], K.Takahashi[2], A. Isayama[2], M. Wanner[3], M. Scannapiego[4], C. Day[4]

[1] *ISTP Istituto di Scienza e Tecnologia del Plasma - CNR, Milano, Italy*
[2] *Fusion Energy R&D Directorate -QST , Naka, Ibaraki, Japan*
[3] *Fusion for Energy, Broader Approach Program, Garching, Germany*
[4] *KIT, Karlsruher Institut für Technologie, Germany*

Introduction. The JT-60SA large superconducting tokamak being jointly built by Europe and Japan [1] under the Broader Approach agreement will start operation in 2020. It is designed to address many areas of fusion science in preparation of the burning plasma of ITER and DEMO, in particular the ones related to the control of high β steady state plasmas and the confinement of high energy particles. A key tool in the machine is the 7 MW, 9 gyrotrons ECRF system which, as for the 34 MW NBI system, will be available at full performance in the Integrated Research Phase. The ECRF system will support plasma operations from the very beginning for EC assisted start-up, EC wall conditioning, bulk heating and later on current drive and magneto-hydrodynamic instabilities control. In order to allow the needed flexibility the ECRF system will operate at three different frequencies, 82, 110 and 138 GHz.

Motivation. An analysis of the residual non-absorbed ECRF power fraction expected in the low absorption plasma scenarios is presented in this contribution, studying its dependence on the steering angle and on the plasma temperature. A fraction of about 5% power in mismatched wave polarization could be expected. Such conditions of low absorption may be relevant during various plasma operation phases, such EC assisted start-up and burn-through, EC wall conditioning or also transiently during events leading to rapid changes in the kinetic profiles and in the magnetic configuration. The distribution of the expected EC stray radiation in the vessel and particularly around some critical areas of the divertor pumping apertures is evaluated. An approach to evaluate the overall EC stray power level is provided by the coupled resonator model (CRM) [3]. However, CRM does not provide the information related to the directivity and inhomogeneity of ECW propagation and absorption. The technique presented here provides a complementary analysis useful in cases in which such aspects play an important role.

Method. An electromagnetic model of the JT-60SA ECRF antenna has been implemented using the GRASP® code [4], which provides the parameters of the EC beams at the launcher according to the steering settings [5]. Fig.1 shows the antenna model in a simplified

representation of the vessel, in which a beam is launched in vacuum towards the centre. Fig.2 is a detail of the divertor region. The propagation of such beams in the plasma is modelled by the GRAY code [6]. The residual non-absorbed EC power fraction has been calculated along the full poloidal steering range.

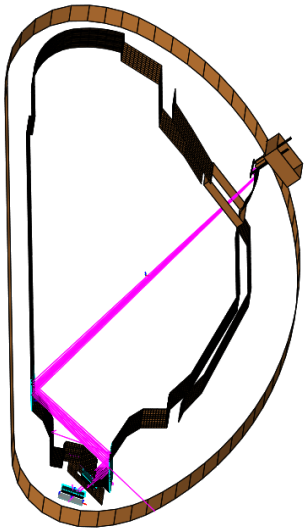

Fig. 1. Beam trajectory in vacuum for launcher settings aiming toward the vessel centre

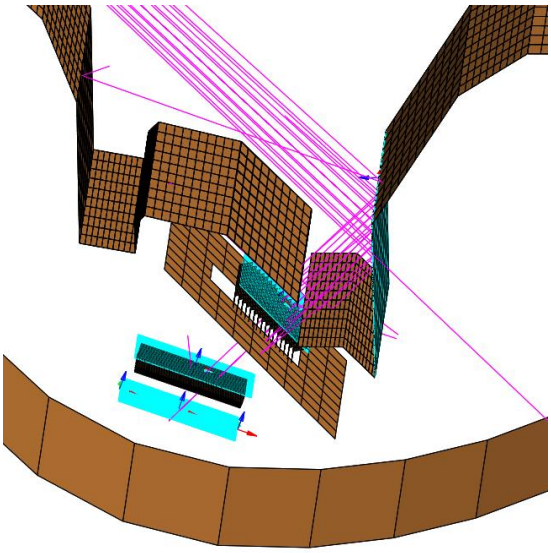

Fig. 2. Beam reflection across the cryopumps aperture below the divertor cassette

The residual non absorbed power after the first and the second pass across the plasma has been evaluated preserving the information of the localization for both XM2 and OM2 polarization modes. The calculation has been performed for plasma kinetic profiles derived from scenario 2 [7] in which the temperature has been reduced such that non absorbed power fraction becomes relevant. While this does not necessarily represent a realistic plasma scenario, it is useful to evaluate the EC stray power level, its distribution in the vessel, its dependence on the launching settings and on the plasma temperature for example during plasma ramp-up and ramp-down. In a second step, the wave propagation outside the plasma, against the first wall and particularly through the divertor pumping apertures and the water baffles of the cryopumps has been calculated with the Physical Optics method of the GRASP® code, keeping into account the amount of residual power fraction. A simplified model of the cryopumping system [8] has been implemented for this purpose, neglecting the toroidal curvature and representing the relevant surfaces as reflectors. This calculation (OPT) is considered as a "worst-case" scenario regarding the local power density and the absorbed power on the water baffles, on the 80K baffles and on the 4K cryopanels (cyan areas in Fig.2).

Results. The distribution of the non-absorbed EC power fraction after 1 and 2 passes across the plasma is shown in Fig.3 for the launched O2M case with perpendicular launch (pure

ECRH). This case represents the fraction of mismatched polarization at launch with respect to the mainly used XM2 mode that has higher absorption coefficient. The color and the size of the symbols represent the residual P/P_0 value. Fig.4 shows the residual EC power (contour lines) after 1 and 2 passes as a function of the poloidal steering angle and of the plasma central temperature. It can be seen that the residual non absorbed power arising from the OM2 fraction is relevant also at relatively high plasma temperatures ~5KeV (top panel), while the XM2 non absorbed is negligible for temperature above 0.1 KeV. The more exposed vessel area is the top of the vessel HFS due to the residual after the first pass, which on the other hand is an unlikely direction of launch. There is, however, significant non absorbed power fraction in the LFS close to the divertor region after the second pass. The calculated power (density) on 4K cryopanels surfaces is reported in table 1, assuming 5% of unmatched polarization content (OM2), 1 MW launched power central plasma temperature of 4-8 keV, absorption coefficient of 0.08 for the first wall, 0.04/0.7 (uncoated/coated) for the water baffles, 0.7 for the 80 K baffles and of 0.08 for the 4K cryopanels.

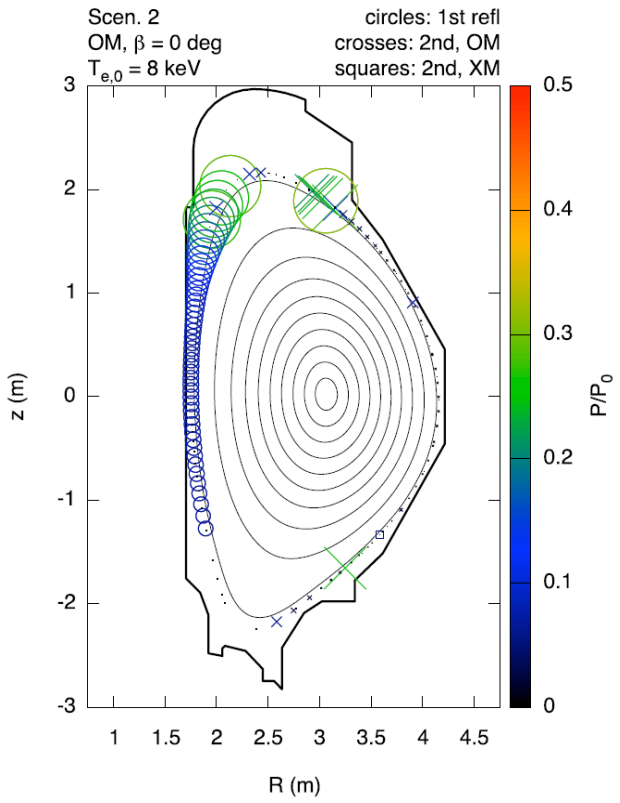

Fig. 3. Pattern of the residual (non-absorbed) ECRF power distribution after 1-2 passes across the plasma for a range of launching angles in the poloidal plane

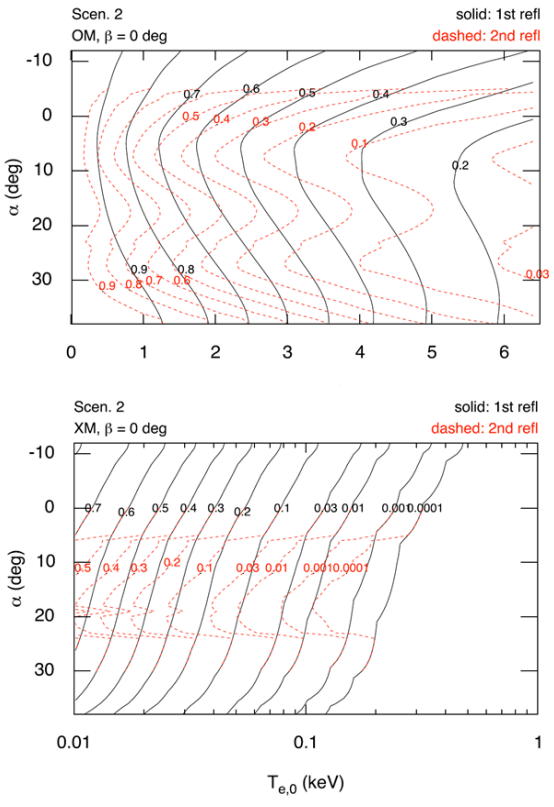

Fig. 4. Contours of the residual power after 1-2 passes as a function of the poloidal injection angle and of the central plasma temperature

The results of OPT are reported in table 1. For comparison, CRM gives 3.067 10^{-3} (9.6 10^{-4}) kWm^{-2} for the uncoated (coated) water baffles case corresponding respectively to 1.371 10^{-2}

(4.292 10^{-3}) of absorbed power. Depending on the plasma scenario, OPT expectations may be 10-30 times higher than CRM on the 4K cryopanels surface. This is coherent with the assumption of directive beam (OPT) rather than the one of randomly scattered radiation taken in CRM. The effect due to the dielectric coating however is more effective in OPT than in CRM, such that the power density on the 4K cryopanels for the coated case is similar in the two models. These last values appear a minor contribution with respect to the design thermal load of the cryopumping system.

Plasma scenario	Central temperature (keV)	Non absorbed fraction after 2nd pass (35° launch)	Incident power density on First wall LFS (kW/m^2)	Absorbed power density on 4K cryopanel (uncoated w.b.) (kW/m^2)	Absorbed power density on 4K cryopanel (coated w.b.) (kW/m^2)	Absorbed power on 4K cryopanel (uncoated w.b.) (kW)	Absorbed power on 4K cryopanel (coated w.b.) (kW)
Scen_2_beta=0_OM	4.040E+00	2.919E-01	1.926E+01	5.518E-02	5.262E-04	2.467E-01	2.353E-03
Scen_2_beta=0_OM	8.060E+00	2.782E-02	1.835E+00	5.258E-03	5.015E-05	2.351E-02	2.242E-04
Scen_2_beta=15_OM	4.040E+00	1.869E-02	1.233E+00	3.533E-03	3.370E-05	1.580E-02	1.507E-04
Scen_2_beta=15_OM	8.060E+00	3.609E-04	2.381E-02	6.821E-05	6.505E-07	3.050E-04	2.909E-06
Scen_4_beta=0_OM	3.984E+00	4.975E-01	3.282E+01	9.403E-02	8.967E-04	4.204E-01	4.010E-03
Scen_4_beta=0_OM	7.950E+00	1.596E-01	1.053E+01	3.017E-02	2.878E-04	1.349E-01	1.287E-03
Scen_4_beta=15_OM	3.984E+00	9.139E-02	6.029E+00	1.727E-02	1.647E-04	7.724E-02	7.366E-04
Scen_4_beta=15_OM	7.950E+00	1.093E-02	7.212E-01	2.066E-03	1.971E-05	9.240E-03	8.811E-05

Table 1. Calculated power density (power) on the surfaces of the 4K cryopanels, for the cases of coated and uncoated water baffles.

.

References

[1] JT-60SA Research Unit, JT-60SA Research Plan, Version 4.0, September 2018, *http://www.jt60sa.org/pdfs/JT-60SA_Res_Plan.pdf*

[2] T. Kobayashi et al., Fusion Eng. and Des, **96-97**, Pages 503 (2015)

[3] H.P. Laqua et al., 28th EPS Conference, ECA **25A** (2001) 1277-1280 and M.Wanner, Report BA_D_28CQ2H https://users.jt60sa.org/?uid=29TB5K&version=v1.0 (unpublished)

[4] K. Pontoppidan, GRASP Technical Description, TICRA, Denmark 2005

[5] P. Platania et al., AIP Conference Proceedings 1689, **090010** (2015)

[6] D. Farina, Fusion Science and Technology 154, **52** (2007)

[7] L. Garzotti et al., Nuclear Fusion 2, **58** (2018)

[8] X. Luo Fusion Engineering and Design 136 (2018) 467–471

Acknowledgement. This work has been carried out within the framework of the EUROfusion Consortium and has received funding from the Euratom research and training programme 2014-2018 and 2019-2020 under grant agreement No 633053. The views and opinions expressed herein do not necessarily reflect those of the European Commission.